

Objective Measures of Neural Processing of Interaural Time Differences

David McAlpine, Nicholas Haywood, Jaime Undurraga
and Torsten Marquardt

Abstract We assessed neural sensitivity to interaural time differences (ITDs) conveyed in the temporal fine structure (TFS) of low-frequency sounds and ITDs conveyed in the temporal envelope of amplitude-modulated (AM'ed) high-frequency sounds. Using electroencephalography (EEG), we recorded brain activity to sounds in which the interaural phase difference (IPD) of the TFS (or the modulated temporal envelope) was repeatedly switched between leading in one ear or the other. When the amplitude of the tones is modulated equally in the two ears at 41 Hz, the interaural phase modulation (IPM) evokes an IPM following-response (IPM-FR) in the EEG signal. For low-frequency signals, IPM-FRs were reliably obtained, and largest for an IPM rate of 6.8 Hz and when IPD switches (around 0°) were in the range 45–90°. IPDs conveyed in envelope of high-frequency tones also generated IPM-FRs; response maxima occurred for IPDs switched between 0° and 180° IPD. This is consistent with the interpretation that distinct binaural mechanisms generate the IPM-FR at low and high frequencies, and with the reported physiological responses of medial superior olive (MSO) and lateral superior olive (LSO) neurons in other mammals. Low-frequency binaural neurons in the MSO are considered maximally activated by IPDs in the range 45–90°, consistent with their reception of excitatory inputs from both ears. High-frequency neurons in the LSO receive excitatory and inhibitory input from the two ears receptively—as such maximum activity occurs when the sounds at the two ears are presented out of phase.

D. McAlpine (✉) · N. Haywood · J. Undurraga · T. Marquardt
UCL Ear Institute, 332 Gray's Inn Road, London WC1X 8EE, UK
e-mail: d.mcalpine@ucl.ac.uk

N. Haywood
e-mail: n.haywood@ucl.ac.uk

J. Undurraga
e-mail: j.undurraga@ucl.ac.uk

T. Marquardt
e-mail: t.marquardt@ucl.ac.uk

© The Author(s) 2016

P. van Dijk et al. (eds.), *Physiology, Psychoacoustics and Cognition in Normal and Impaired Hearing*, Advances in Experimental Medicine and Biology 894, DOI 10.1007/978-3-319-25474-6_21

Keywords Interaural phase modulation · Objective measures · Frequency-following response · Electroencephalography

1 Introduction

1.1 *Advantages of Binaural Listening*

Binaural hearing confers considerable advantages in everyday listening environments. By comparing the timing and intensity of a sound at each ear, listeners can locate its source on the horizontal plane, and exploit these differences to hear out signals in background noise—an important component of ‘cocktail party listening’. Sensitivity to interaural time differences (ITDs) in particular has received much attention, due in part to the exquisite temporal performance observed; for sound frequencies lower than about 1.3 kHz, ITDs of just a few tens of microseconds are discriminable, observed both at the neural and behavioural levels. Sensitivity to ITDs decreases with ageing (Herman et al. 1977; Abel et al. 2000; Babkoff et al. 2002), and is typically impaired in hearing loss, albeit variability across individuals and aetiologies (see Moore et al. 1991, for review), with reduced sensitivity most apparent when trying to localise sources in background noise (Lorenzi et al. 1999). ITD processing may also remain impaired following surgery to correct conductive hearing loss (Wilmington et al. 1994), and sensitivity to ITDs is typically poor in users of hearing technologies such as bilateral cochlear implants (CIs). In terms of restoring binaural function in therapeutic interventions, there is considerable benefit to be gained from developing objective measures to assess binaural processing.

1.2 *Objective Measures of Binaural Hearing*

Direct measures of ITD sensitivity, attributed to multiple generator sites in the thalamus and auditory cortex (Picton et al. 1974; Hari et al. 1980; Näätänen and Picton 1987; Liégeois-Chauvel et al. 1994), have been demonstrated in auditory-evoked ‘P1-N1-P2’ responses, with abrupt changes in either the ITD (e.g. McEvoy 1991), or the interaural correlation of a noise (e.g. Chait et al. 2005), eliciting responses with typical latencies of 50, 100, and 175 ms, respectively. Although these studies demonstrate the capacity to assess binaural processing of interaural temporal information, they provide for only a relatively crude measure of ITD sensitivity, comparing, for example, EEG responses to diotic (identical) sounds at the two ears with responses to sounds that are statistically independent at the two ears. A more refined measure of ITD sensitivity would provide the possibility of assessing neural mechanisms of binaural processing in the human brain, aiding bilateral fitting of CIs in order to maximise binaural benefit.

2 Methods

Eleven NH listeners took part in the low-frequency EEG experiment (6 male; mean age=24.4 years, range=18–34 years). Four listeners took part in the high-frequency experiment (3 male; mean age=30.0 years, range=27–34 years). All subjects demonstrated hearing levels of 20 dB hearing level or better at octave frequencies between 250 and 8000 Hz, and reported a range of musical experience. Subjects were recruited from poster advertisements. All experiments were approved by the UCL Ethics Committee. Subjects provided informed consent, and were paid an honorarium for their time. For EEG recordings assessing sensitivity to ITDs in the low-frequency TFS, 520-Hz carrier tones were modulated with 100% sinusoidal AM (SAM), at a rate of 41 Hz. Stimuli were presented continuously for 4 min and 48 s (70 epochs of 4.096 s) at 80 dB SPL. Carrier and modulation frequencies were set so that an integer number of cycles fitted into an epoch window. The carrier was presented with an IPD (in the range $\pm 11.25^\circ$ – $\pm 135^\circ$ IPD around 0°), whilst the modulation envelope remained diotic at all times. In order to generate IPM, the overall magnitude of the carrier IPD was held constant throughout the stimulus, but the ear at which the signal was leading in phase was periodically modulated between right and left. Each IPM was applied instantaneously at a minimum in the modulation cycle in order to minimize the (monaural) salience of the instantaneous phase transition (see Fig. 1). Stimuli were AM'ed at a rate of 41 Hz. The IPD cycled

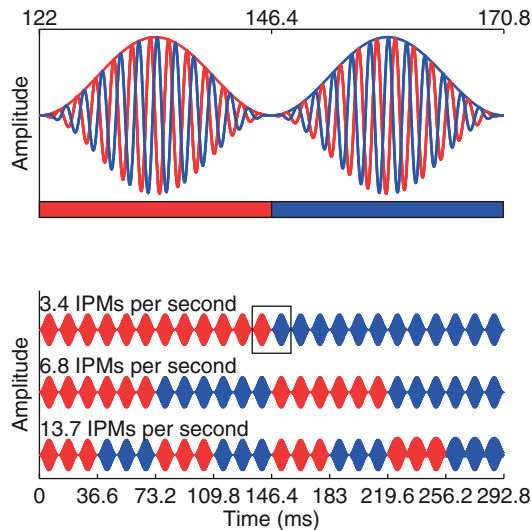


Fig. 1 AM stimuli presented to each ear. *Top panel*, red and blue correspond to sounds presented to right and left ears, respectively. Filled horizontal bars indicate the ear with leading phase. The IPD of this example corresponds to $\pm 90^\circ$ (switching from -45 to 45° , and vice versa, in the two ears). IPD transitions are introduced when the stimulus amplitude is zero. *Bottom panel*, three IPM rates employed. Red regions illustrate an IPD of $+90^\circ$ IPD, whereas blue regions illustrate an IPD of -90° IPD. IPM rate is controlled by the number of AM cycles where the IPD is held constant

periodically at three different rates: 1.7, 3.4 and 6.8 Hz, referred as IPD cycle rates. However, since responses were expected to be elicited by each IPD transition, we refer to the stimulus largely in terms of IPM rate, which indicates the total number of IPD transitions per second, irrespective of direction. Thus, the three IPM rates tested were: 3.4, 6.8 and 13.7 Hz. These IPM rates corresponded to an IPD transition every 12, 6 and 3 AM cycles, respectively (Fig. 1).

For EEG recordings to ITDs conveyed in the stimulus envelope, 3000-Hz tones were modulated with a transposed envelope (Bernstein and Trahiotis 2002) at 128 Hz, and a second-order AM (41 Hz) applied diotically. IPDs of the 128-Hz envelopes were switched between $\pm 90^\circ$ IPD (around 0°) or from systematically between 0° and 180° (i.e. transposed phase of -90° in one ear and $+90^\circ$ in the other).

Stimuli were created in Matlab, and presented by an RME Fireface UC sound card (24 bits, 48 kHz sampling rate) connected to Etymotic Research ER-2 insert earphones. Sound level was verified with a 2-cc B&K artificial ear. EEG responses were recorded differentially from surface electrodes; the reference electrode was placed on the vertex (Cz), and the ground electrode on the right clavicle. Two recording electrodes were placed on the left and right mastoid (TP9 and TP10). Electrode impedances were kept below 5 k Ω . Responses were amplified with a 20x gain (RA16LI Tucker-Davis Technologies), and digitalized at a rate of 24.414 kHz, and a resolution of 16 bits/sample (Medusa RA16PA Tucker-Davis Technologies). The cutoff frequencies of the internal bandpass filter were 2.2 and 7.5 kHz, respectively (6 dB per octave). Recordings were next stored on a RX5 Pentium before being passed to hard disk via custom software. Recordings were processed off-line using Matlab.

During the experiment, subjects sat in a comfortable chair in an acoustically isolated sound booth, and watched a subtitled film of their choice. Subjects were encouraged to sit as still as possible, and were offered a short break every 15–20 min. Epochs of each measurement were transformed to the frequency domain (fast Fourier transform (FFT) of 100,000 points; 0.24 Hz of resolution) and FFTs from all epochs were averaged. Six frequency bins were tested for significance; corresponding to the IPD cycle rate and the next four harmonics, as well as the frequency bin corresponding to the AM rate.

3 Results

3.1 *Sensitivity to IPDs Conveyed in the Temporal Fine Structure of Low-Frequency Sounds*

EEG recordings were obtained for three IPM rates (3.4, 6.8 and 13.7 Hz) and seven IPMs ($\pm 11.25^\circ$, $\pm 22.5^\circ$, $\pm 45^\circ$, $\pm 67.5^\circ$, $\pm 90^\circ$, $\pm 112.5^\circ$ and $\pm 135^\circ$), generating a total of 30 conditions (21 dichotic, 9 diotic), each lasting ≈ 5 min, giving a total recording time of 2.5 h. Figure 2 plots the spectral magnitude of a typical recording for a dichotic condition with IPM of $\pm 67.8^\circ$ and IPM rate of 6.8 Hz, in which a

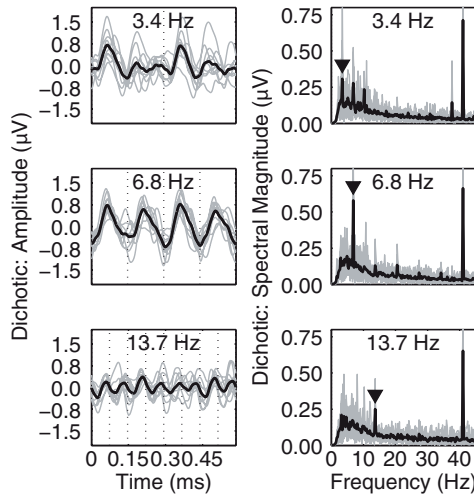


Fig. 2 Average (*thick line*) responses in time and frequency domains to dichotic stimuli, with individual responses shown in *thin gray lines*. Time domain responses are shown in *left panels* and frequency responses in *right panels*. Responses to *low, middle and high IPM rates* (3.4, 6.8 and 13.7 Hz) in *top, middle, and bottom rows*. All responses correspond to the $\pm 67.8^\circ$ IPD condition. *Dashed vertical lines* in time-domain responses indicate the time of the IPD transition. Black markers in the frequency domain indicate IPM rate

significant response was observed for the frequency bin corresponding to the IPM rate (black arrow), and corresponding diotic conditions are shown in Fig. 3—for which no response to the IPM rate was observed (see Ross 2008). Note that in both conditions the ASSR to the AM rate (41 Hz) was clearly observed.

Fig. 3 Average (*thick line*) responses in time and frequency domains to diotic stimuli. Data are plotted in a manner consistent with Fig. 2

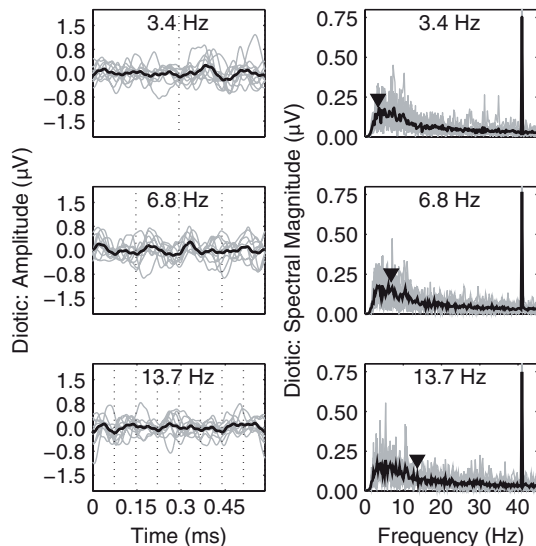


Figure 2 shows responses analysed in the time domain (left panels) and the frequency domain (right) for a single IPM condition ($\pm 67.8^\circ$). Individual (gray lines) and group mean (black) for the slowest IPM rate (3.4 Hz; Fig. 3, *top*), typically displayed a P1-N1-P2 response to each IPD transition, with component latencies of approximately 50, 100 and 175 ms, respectively. The next two harmonics (6.8 and 10.2 Hz) were also observed clearly in the response to the 3.4-Hz IPM. Evoked responses to the intermediate IPM rate (6.8 Hz; Fig. 2) became steady state at the same rate as the IPM, and so we term this response the IPM-FR. In the time domain (left-middle), the peak amplitude of the IPM-FR is broadly the same as that for the slowest IPM rate (3.2 Hz), but responses were more steady state than those at the low rate, being more consistent in phase and amplitude across epochs (evidenced by a more favourable SNR). This is confirmed by comparing the variability of the individual responses in the time domain as well as the frequency domain (Fig. 2), where the spectral magnitude was almost twice larger than that the largest magnitude obtained at the lowest IPM rate. Moreover, the average spectral magnitude of the next harmonics was almost twice smaller than those obtained at the lowest IPM rate. Finally, the IPM-FR is observed at the most rapid IPM rate (13.7 Hz, bottom panels of Fig. 3). As for the intermediate IPM rate, responses show a steady-state pattern in the time domain, albeit with a reduced amplitude. Frequency domain analysis revealed the following response occurred primarily at the frequency bin corresponding to the IPM rate. Harmonics were no longer observed in the grand averaged data.

For analysis of data in the frequency domain, Hotelling's T2 tests were applied to the frequency bins corresponding to the IPM rate and the next four harmonics. Responses were classified as significant if either the left (Tp9), right (Tp10), or both electrodes observed a significant response for a given frequency bin. The frequency bin corresponding to the IPM rate (second harmonic) elicited the highest number of significant responses. Indeed, responses obtained at IPM rates of 6.8 and 13.7 Hz were observed for all ten subjects for the $\pm 45^\circ$ and $\pm 135^\circ$ IPD conditions, respectively. This was not the case for the lowest IPM rate where significant responses were observed for only seven subjects. In terms of spectral magnitude, responses obtained at the intermediate IPM rate showed the largest magnitude at the second harmonic, i.e. the harmonic corresponding to the IPM rate, consistent with the hypothesis that a following-response (FR) is evoked by IPM.

Finally, we assessed the frequency bin corresponding to the IPM rate. A three-way non-parametric repeated measures ANOVA with factors of electrode position (left or right mastoid), IPM rate, and IPD revealed that factors IPM rate ($p < 0.001$), IPD ($p < 0.001$) as well as the interaction between IPM rate and IPD ($p = 0.01$) were significant. Responses obtained at 6.8 Hz IPM rate were maximal for IPDs spanning $\pm 45^\circ$ – $\pm 90^\circ$, whereas responses obtained at 13.4 Hz IPM rate increased monotonically with increasing IPD.

3.2 Sensitivity to IPDs Conveyed in the Temporal Envelope of High-Frequency Sounds

In contrast to low-frequency tones, the magnitude of the IPM-FR for IPDs conveyed in the modulated envelopes of high-frequency (3-kHz) tones was relatively low for IPMs switching between $\pm 90^\circ$ IPD. Therefore, we also assessed EEG responses to IPMs switching between 0° (in phase) and 180° (anti-phasic) IPD conditions. These latter switches evoked considerably larger EEG responses (Fig. 4, *left*). The magnitude of the IPM-FR decreased with increasing carrier frequency, and was sensitive to an offset in the carrier frequency between the ears (Fig. 4, *right*).

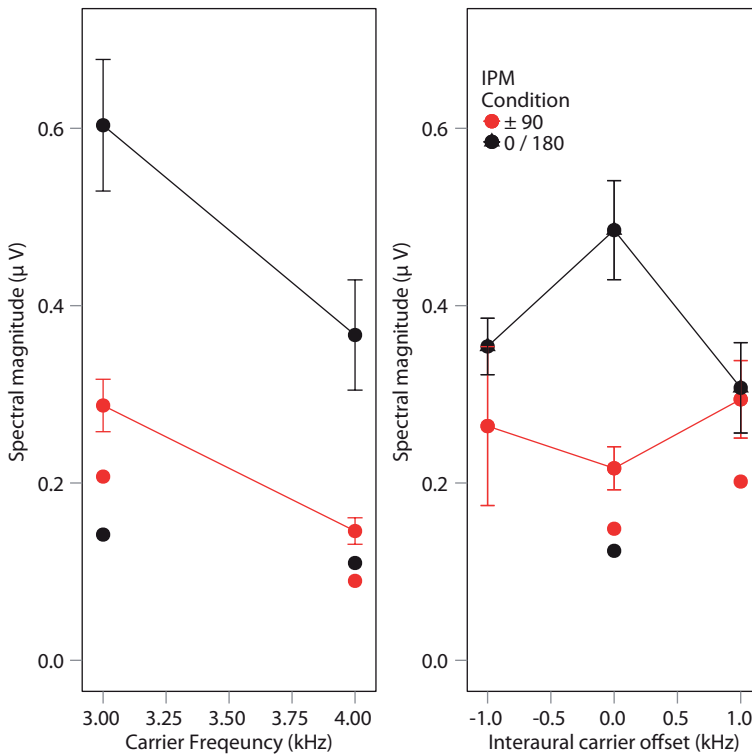


Fig. 4 *Left*—magnitude of IPM-FRs to 3-kHz transposed tones in which envelope IPDs were switched between $\pm 90^\circ$, or between 0° and 180° (transposed phase of 90° at one and -90° at the opposite ear). *Right*—magnitude of IPM-FR as a function of carrier frequency mismatch. In both plots, unconnected symbols indicate response magnitude in equivalent diotic control conditions

4 Discussion

We have demonstrated that an IPM-FR can be reliably obtained and used as an objective measure of binaural processing. Depending on the IPM rate, periodic IPMs can evoke a robust steady-state following response. This is consistent with previous reports that an abrupt change in carrier IPD evokes a P1-N1-P2 transient response (Ross et al. 2007a, b; Ross 2008), and with evidence that abrupt periodic changes in interaural correlation evoked steady-state responses (Dajani and Picton 2006; Massoud et al. 2011). The data also demonstrate that the magnitude of the IPM-FR varies with both the IPM rate and the magnitude of the carrier IPD. As diotic carrier phase modulation did not elicit detectable neural responses, the observed responses to IPM must reflect binaural processing rather than the monaural encoding of abrupt phase shifts (Ross et al. 2007a, b; Ross 2008). The time-domain response waveforms are consistent with evoked responses occurring in cortical and sub-cortical sources along the auditory pathway, and that they originate from superposition of transient middle-latency responses (Galambos et al. 1981).

The difference in the preferred IPDs for EEG signals conveying IPDs in the low-frequency TFS and the modulated envelopes of high-frequency tones is consistent with the underlying physiological mechanisms of neurons in the brainstem pathways sub-serving these two cues. Low-frequency binaural neurons in the MSO and midbrain (inferior colliculus) are maximally activated by IPDs in the range 45–90° (see Grothe et al. 2010 for review). This is consistent with their delay sensitivity being generated by largely excitatory inputs from the two ears. Conversely, those in the LSO appear to be excited by one ear, and inhibited by the other (Grothe et al. 2010). Consequently, maximum activity is generated in this (high-frequency) pathway when the sounds at the two ears are out of phase with each other (here, when the signal is switched from 0° to 180°). The IPM-FR, therefore, appears able to distinguish between these two pathways based on the preferred IPDs employed to evoke the response. This provides a possible means of distinguishing which of the binaural pathways is activated in bilateral CI users, as well as a means of objective fitting of devices. Work is currently underway to assess the IPM-FR in bilateral CI users. The EEG recording of steady-state responses in CI users is made challenging by the electrical artefacts created by stimulus pulses, but artefact rejection techniques have been successfully applied for the recording of AM-evoked steady-state responses (e.g., Hofmann and Wouters 2010). Such techniques should also be applicable for the recording of the IPM-FR.

Acknowledgments This work is supported by the European Commission under the Health Theme of the 7th Framework Programme for Research and Technological Development.

Open Access This chapter is distributed under the terms of the Creative Commons Attribution-Noncommercial 2.5 License (<http://creativecommons.org/licenses/by-nc/2.5/>) which permits any noncommercial use, distribution, and reproduction in any medium, provided the original author(s) and source are credited.

The images or other third party material in this chapter are included in the work's Creative Commons license, unless indicated otherwise in the credit line; if such material is not included in the work's Creative Commons license and the respective action is not permitted by statutory regulation, users will need to obtain permission from the license holder to duplicate, adapt or reproduce the material.

References

- Abel SM, Giguère C, Consoli A, Papsin BC (2000) The effect of aging on horizontal plane sound localization. *J Acoust Soc Am* 108:743–52
- Babkoff H, Muchnik C, Ben-David N, Furst M, Even-Zohar S, Hildesheimer M (2002) Mapping lateralization of click trains in younger and older populations. *Hear Res* 165:117–27
- Bernstein LR, Trahiotis C (2002) Enhancing sensitivity to interaural delays at high frequencies by using transposed stimuli. *J Acoust Soc Am* 122:1026–1036
- Chait M, Poeppel D, de Cheveigné A, Simon JZ (2005) Human auditory cortical processing of changes in interaural correlation. *J Neurosci* 25:8518–27
- Dajani HR, Picton TW (2006) Human auditory steady-state responses to changes in interaural correlation. *Hear Res* 219:85–100
- Galambos R, Makeig S, Talmachoff PJ (1981) A 40-Hz auditory potential recorded from the human scalp. *Proc Natl Acad Sci U S A* 78:2643–2647
- Grothe B, Pecka M, McAlpine D (2010) Mechanisms of sound localization in mammals. *Physiol Rev* 90:983–1012
- Hari R, Aittoniemi K, Järvinen ML, Katila T, Varpula T (1980) Auditory evoked transient and sustained magnetic fields of the human brain. Localization of neural generators. *Exp Brain Res* 40:237–240
- Herman GE, Warren LR, Wagener JW (1977) Auditory lateralization: age differences in sensitivity to dichotic time and amplitude cues. *J Gerontol* 32(2):187–191. doi: 10.1093/geronj/32.2.187
- Hofmann M, Wouters J (2010) Electrically evoked auditory steady state responses in cochlear implant users. *J Assoc Res Otolaryngol* 11:267–282
- Liégeois-Chauvel C, Musolino A, Badier JM, Marquis P, Chauvel P (1994) Evoked potentials recorded from the auditory cortex in man: evaluation and topography of the middle latency components. *Electroencephalogr Clin Neurophysiol* 92:204–214
- Lorenzi C, Gatehouse S, Lever C (1999) Sound localization in noise in hearing-impaired listeners. *J Acoust Soc Am* 105:3454–3463
- Massoud S, Aiken SJ, Newman AJ, Phillips DP, Bance M (2011) Sensitivity of the human binaural cortical steady state response to interaural level differences. *Ear Hear* 32:114–120
- McEvoy LK, Picton TW, Champagne SC (1991) Effects of stimulus parameters on human evoked potentials to shifts in the lateralization of a noise. *Audiology* 30:286–302
- Moore DR, Hutchings ME, Meyer SE (1991) Binaural masking level differences in children with a history of otitis media. *Audiology* 30:91–101
- Näätänen R, Picton T (1987) The N1 wave of the human electric and magnetic response to sound: a review and an analysis of the component structure. *Psychophysiology* 24:375–425
- Picton TW, Hillyard SA, Krausz HI, Galambos R (1974) Human auditory evoked potentials. I. Evaluation of components. *Electroencephalogr Clin Neurophysiol* 36:179–190
- Ross B (2008) A novel type of auditory responses: temporal dynamics of 40-Hz steady-state responses induced by changes in sound localization. *J Neurophysiol* 100:1265–1277
- Ross B, Fujioka T, Tremblay KL, Picton TW (2007a) Aging in binaural hearing begins in mid-life: evidence from cortical auditory-evoked responses to changes in interaural phase. *J Neurosci* 27:11172–11178
- Ross B, Tremblay KL, Picton TW (2007b) Physiological detection of interaural phase differences. *J Acoust Soc Am* 121:1017
- Wilmington D, Gray L, Jahrsdoerfer R (1994) Binaural processing after corrected congenital unilateral conductive hearing loss. *Hear Res* 74(1-2):99–114